

PARTICLE DETECTION AND VELOCITY MEASUREMENT IN LASER DOPPLER VELOCIMETRY USING KALMAN FILTERS

Alain Le Duff, Guy Plantier and Anthony Sourice

École Supérieure d'Électronique de l'Ouest - 4 Rue Merlet de la Boulaye - BP 30926 - 49009 Angers cedex 01 - France.

ABSTRACT

This paper discusses a processing technique for LDV data, based on the use of two Kalman filters, enabling to detect the presence of particles and to infer their velocity. This method turns out to be suitable for the design of real-time integrated velocimeters. A first estimator, based on the use of a Kalman filter, deals with the amplitude of the Doppler signal. A second one, using an Extended Kalman Filter, allows particle velocity estimation which is assumed to be a constant. Finally, the estimator is studied by means of Monte Carlo trials obtained from synthesized signals, and its performance is then compared to the Cramer-Rao bound.

1. INTRODUCTION

Laser Doppler Velocimetry (LDV) is a non-invasive technique for measuring the particle velocity in a fluid by laser interferometry. This technique has been widely used for many years for fluid flow measurements thanks to several advantages: LDV allows contactless measurements, uses a small measuring volume giving an excellent spatial resolution, and has a linear response. However, conventional LDV has two main drawbacks: at first, its complexity requires a substantial know-how for an efficient use, and then, such a system is expensive. In order to design more integrated a set-up, providing accurate real-time measurements of particle velocity with low sampling frequency, the use of an Extended Kalman Filter (EKF), for a baseband signal in quadrature, is proposed. Moreover, prior to estimation, it is necessary to detect whether a particle is currently in the laser velocimeter or not. This detection is performed by comparing the amplitude of the Doppler signal, estimated thanks to a Kalman filter, with a threshold. It should be noted that, in order to eliminate the need for storing all the past observed data, a recursive Kalman filter is more efficient than a classical post-processing scheme [3, 4] like the Maximum Likelihood Estimator (MLE) [1, 7] or time-frequency methods [8, 9] for example.

This article is organized as follows: in section 2, the principles of Laser Doppler Velocimetry are presented and the experimental set-up is described. In Section 3, a model for the Doppler signal is proposed. The detection scheme is

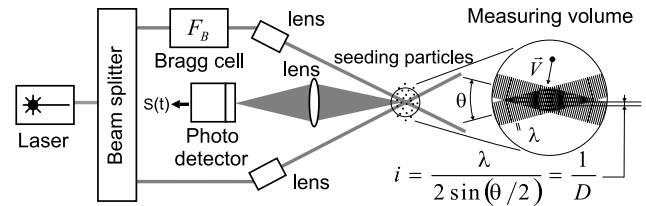


Fig. 1. Description of the LDV system.

presented in section 4. Section 5 deals with velocity estimation, and finally, in Section 6, numerical examples illustrate the performance of the method and a statistical analysis of the estimations, by means of Monte-Carlo simulations, is given.

2. LDV PRINCIPLES

A typical LDV system is described in figure 1. Two laser beams, crossed and focused, define a measuring volume in which an interference pattern, made of bright and dark fringes, appears. The spacing between two adjacent bright fringes, i , depends on the wavelength of the laser light, λ , and on the angle between both beams, θ :

$$i = \frac{\lambda}{2 \sin(\theta/2)}. \quad (1)$$

The quantity $D = 1/i$ represents the sensitivity of the set-up. A seeding particle scatters light while crossing this volume. This light is then detected by a photo-detector and its intensity is modulated with a frequency equal to

$$F_D = \frac{V}{i} = DV = \frac{2 \sin(\theta/2)}{\lambda} V, \quad (2)$$

where V is the component of the velocity \vec{V} perpendicular to the fringes, λ the laser wavelength and θ the angle between beams. In order to avoid any ambiguity on velocity sign, the interference fringes are shifted with the help of a Bragg cell at $F_B = 40$ MHz. Finally, the signal is down shifted thanks to an analog Quadrature Demodulation (QD) technique, as shown in figure 2. Consequently, an estimation of F_D leads to an estimation of the velocity. Then, F_D

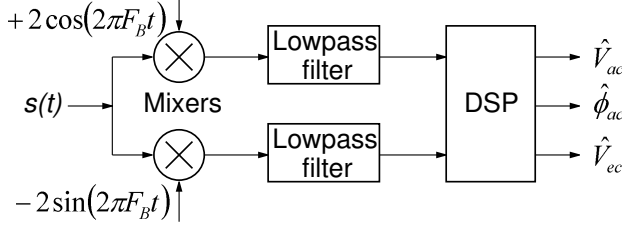


Fig. 2. Schematic diagram of quadrature demodulation technique.

determination allows velocity estimation. Additional principles of LDV can be found in [2].

3. SIGNAL MODEL

For our demonstration, it is assumed that only one particle is present in the measuring volume with a constant velocity V . Then the electrical signal delivered by the photo-detector is

$$s(t) = A(t) \{M + \cos[2\pi(F_B + F_D)t + \phi_0]\} \quad (3)$$

$$s(t) = A(t) \{M + \cos[2\pi F_B + 2\pi D x(t) + \phi_0]\} \quad (4)$$

In this equation, $A(t)$ and $x(t)$ represent, respectively, the amplitude and the position of the particle at the instant t , with $A(t) = K e^{-\{\beta x(t)\}^2}$ and $x(t) = V(t - t_0)$. K represents the maximum amplitude of $s(t)$ (K results from optical power and particle area section), and $1/\beta$ defines the width of the probe volume. t_0 denotes the time when the particle reaches the center of the measuring volume. In (3), the constant M is due to the difference between the intensities of both beams. This offset, weighted by the gaussian shape $A(t)$, is called *burst pedestal* ($M A(t)$). Moreover, it should be noted that the time support of the signal, and therefore the duration of the burst, depends on particle velocity. Thus, the Doppler signal is roughly a sine-wave at frequency $F_B + F_D$ with a time-varying amplitude $A(t)$. The offset component M is then eliminated by an electrical high-pass filter. After applying the QD technique (figure 2) the following sine/cosine pair $s_1(t) = A(t) \cos \phi(t)$ and $s_2(t) = A(t) \sin \phi(t)$ are obtained, with $\phi(t) = 2\pi D x(t) + \phi_0$. After sampling, the discrete-time measured signals are given by $y_1(kT_e)$ and $y_2(kT_e)$ where T_e is the sampling period (in the rest of this document, the following notations $y_1(kT_e) = y_1(k)$ and $y_2(kT_e) = y_2(k)$ are used). Hence, one can write

$$y_1(k) = A(k) \cos \phi(k) + v_1(k) \quad (5)$$

$$y_2(k) = A(k) \sin \phi(k) + v_2(k). \quad (6)$$

In these relations, $\phi(k) = 2\pi D x(k) + \phi_0$ represents the instantaneous phase with $x(k) = V(kT_e - t_0)$, $v_1(k)$ and $v_2(k)$ are sequences of zero-mean independent gaussian random variables with variance σ^2 . The goal of signal proces-

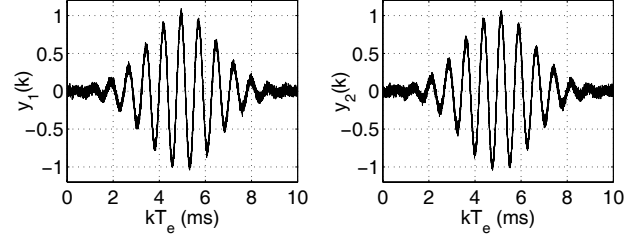


Fig. 3. Doppler signal for $V = 10$ mm/s (SNR = 27 dB).

sing is then to extract the particle velocity V from the observed signals $y_1(k)$ and $y_2(k)$. As an example, figure 3 shows a simulated Doppler signal in the case of a 10mm/s velocity with a 27dB Signal-to-Noise Ratio (SNR). The SNR is defined as

$$SNR = 10 \log_{10} (K^2/2\sigma^2). \quad (7)$$

4. DETECTION OF PARTICLES ARRIVAL

The detection scheme is based on the use of a trigger which compares the estimated amplitude of the Doppler signal with a threshold. If noise is taken into account, the magnitude of the Doppler signal is then equal to

$$A_b(k) = \sqrt{y_1^2(k) + y_2^2(k)} \quad (8)$$

$$= \sqrt{[s_1(k) + b_1(k)]^2 + [s_2(k) + b_2(k)]^2}. \quad (9)$$

The Probability Density Function (PDF) of $A_b(k)$ is then given by [6]

$$p[A_b(k)] = \frac{A_b(k)}{\sigma^2} \exp \left[-\frac{A_b^2(k) + A^2(k)}{2\sigma^2} \right] I_0 \left[\frac{A_b(k)A(k)}{\sigma^2} \right] \quad (10)$$

where $A(k) = \sqrt{s_1^2(k) + s_2^2(k)}$ is the real amplitude of the signal and $I_0(u) = \frac{1}{2\pi} \int_0^{2\pi} \exp(u \cos \phi) d\phi$ is the modified Bessel function of the first kind and order 0 [6]. When no particle is present in the measuring volume, $A(k) = 0$. Then, $y_1(k) = v_1(k)$, $y_2(k) = v_2(k)$ and (10) is reduced to the Rayleigh PDF, the mean of which is

$$E[A_b(k)] = K_1 = \sqrt{\frac{\pi\sigma^2}{2}} = 1.25\sigma. \quad (11)$$

In addition to that, for large SNR values (*i.e.* when $A(k)$ is high), (10) looks like a gaussian PDF. Hence, the mean of this estimated amplitude is close to the true amplitude:

$$E[A_b(k)] \equiv A(k). \quad (12)$$

The figure 4 shows the evolution of the mean $E[A_b(k)]$ versus $A(k)$. The amplitude of the signal can be modeled as

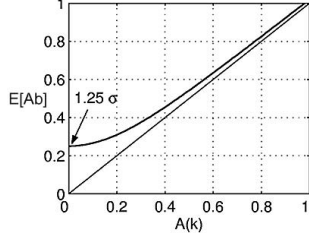


Fig. 4. Evolution of the mean $E[A_b(k)]$ versus $A(k)$.

the sum of a constant $K_1 = 1.25\sigma$ and a time varying component $K_2(k)$ close to $A(k)$ when the SNR is large enough.

$$A_b(k) = K_1 + K_2(k). \quad (13)$$

The amplitude estimator should be robust to modeling errors; thus, $K_2(k)$ can be modeled using a random walk. Consequently, the state space representation of (5) and (6) can be written as follows:

$$\mathbf{X}_1(k+1) = \mathbf{A}_1 \mathbf{X}_1(k) + \mathbf{W}_1(k) \quad (14)$$

$$\mathbf{Y}_1(k) = \mathbf{C}_1 \mathbf{X}_1(k) + \mathbf{V}_1(k) \quad (15)$$

where the state vector $\mathbf{X}_1(k)$, the measurement vector $\mathbf{Y}_1(k)$ (observed data), the state transition matrix \mathbf{A}_1 and the measurement matrix \mathbf{C}_1 are

$\mathbf{X}_1(k) = [x_1(k), x_2(k)]^T = [K_1, K_2(k)]^T$,
 $\mathbf{Y}_1(k) = [\sqrt{y_1^2(k) + y_2^2(k)}]$, $\mathbf{A}_1 = \begin{bmatrix} 1 & 0 \\ 0 & 1 \end{bmatrix}$, $\mathbf{C}_1 = [1, 1]$. $\mathbf{W}_1(k) = [0, w(k)]^T$ and $\mathbf{V}_1(k) = v(k)$ are, respectively, process and measurement noises which are white and zero-mean noises with variances σ_w^2 and σ_v^2 . These noise vectors are statistically independent. Based on (14) and (15) and from the initial conditions ($\mathbf{P}(0|-1) = \mathbf{P}_0$ and $\hat{\mathbf{X}}(0|-1) = (0)$), we can recursively calculate the mean, $\hat{\mathbf{X}}(k|k)$, and the covariance, $\mathbf{P}(k|k)$, thanks to the Kalman filter recursions: $k = 1, 2, 3, \dots$

$$\begin{aligned} \mathbf{L}_1(k) &= \mathbf{P}_1(k|k-1) \times \\ &\quad \mathbf{C}_1^T \left\{ \mathbf{C}_1 \mathbf{P}_1(k|k-1) \mathbf{C}_1^T + \mathbf{R}_{1V}(k, k) \right\}^{-1} \\ \hat{\mathbf{X}}_1(k|k) &= \hat{\mathbf{X}}_1(k|k-1) + \\ &\quad \mathbf{L}_1(k) [\mathbf{Y}_1(k) - \mathbf{C}_1 \hat{\mathbf{X}}_1(k|k-1)] \\ \mathbf{P}_1(k|k) &= \mathbf{P}_1(k|k-1) - \mathbf{L}_1(k) \mathbf{C}_1 \mathbf{P}_1(k|k-1) \\ \hat{\mathbf{X}}_1(k+1|k) &= \mathbf{A}_1 \hat{\mathbf{X}}_1(k|k) \\ \mathbf{P}_1(k+1|k) &= \mathbf{A}_1 \mathbf{P}_1(k|k) \mathbf{A}_1^T + \mathbf{R}_{1W}(k, k). \end{aligned}$$

For example, figure 5 (left) shows the result of an estimation of K_1 (—) and $E[A_b(k)]$ (—) i.e. the mean of the amplitude of the Doppler signal. The detection is then performed by comparing $E[A_b(k)]$ to a threshold $K_{th} = 1.5 \times \hat{K}_1$ as shown in figure 5 (right). When the amplitude of the Doppler signal is greater than K_{th} , it can be inferred that a particle is present in the measuring volume and that the observed signal is containing meaningful information.

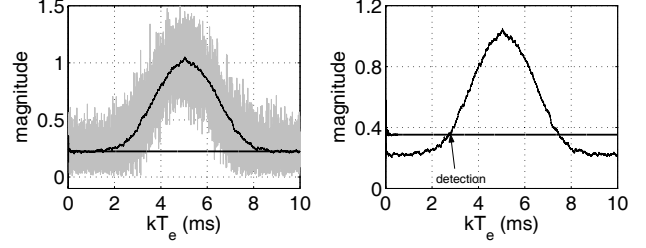


Fig. 5. (left) Estimation of K_1 (—) and $E[A_b(k)]$ (—) the mean of the amplitude of the Doppler signal. The real amplitude is in gray. (right) Detector threshold (—) and $E[A_b(k)]$ (—) ($V = 10$ mm/s, SNR = 12 dB).

5. PARTICLE VELOCITY ESTIMATION

After triggering, i.e. if a particle has entered in the measuring volume, it is possible to estimate particle velocity. This estimation is achieved thanks to an EKF. The state space representation of the Doppler signal is then given by

$$\mathbf{X}_2(k+1) = \mathbf{A}_2 \mathbf{X}_2(k) + \mathbf{W}_2(k) \quad (16)$$

$$\mathbf{Y}_2(k) = G[k, \mathbf{X}_2(k)] + \mathbf{V}_2(k) \quad (17)$$

with the state vector $\mathbf{X}_2(k) = [x_1(k), x_2(k)]^T = [\phi(k), V]^T$ and the state transition matrix $\mathbf{A}_2 = \begin{bmatrix} 1 & 2\pi D T_e \\ 0 & 1 \end{bmatrix}$.

$\mathbf{W}_2(k)$ and $\mathbf{V}_2(k)$ are, respectively, process and measurement noises which are white and zero-mean statistically independent noises. In this case, the measurement equation (17), described by (5) and (6), is highly non-linear. In order to use a Kalman filter, these equations should be linearized by means of a first order Taylor development around $\mathbf{X}_2(k)$. The measurement matrix is then given by

$$\begin{aligned} \mathbf{C}_2(k+1) &= \left. \frac{\partial G[k+1, \mathbf{X}_2(k)]}{\partial \mathbf{X}_2(k)} \right|_{\mathbf{X}_2(k)} \\ &= \begin{bmatrix} -A(k+1) \sin[\hat{x}_1(k+1|k)] \\ +A(k+1) \cos[\hat{x}_1(k+1|k)] \end{bmatrix} \end{aligned} \quad (18)$$

where $A(k)$ is assumed to be known and close to $E[A_b(k)]$. Then, the EKF can be summarized as: $k = 1, 2, 3, \dots$

$$\begin{aligned} \mathbf{L}_2(k) &= \mathbf{P}_2(k|k-1) \times \\ &\quad \mathbf{C}_2^T \left\{ \mathbf{C}_2 \mathbf{P}_2(k|k-1) \mathbf{C}_2^T + \mathbf{R}_{2V}(k, k) \right\}^{-1} \\ \hat{\mathbf{X}}_2(k|k) &= \hat{\mathbf{X}}_2(k|k-1) + \\ &\quad \mathbf{L}_2(k) [\mathbf{Y}_2(k) - \mathbf{C}_2 \hat{\mathbf{X}}_2(k|k-1)] \\ \mathbf{P}_2(k|k) &= \mathbf{P}_2(k|k-1) - \mathbf{L}_2(k) \mathbf{C}_2 \mathbf{P}_2(k|k-1) \\ \hat{\mathbf{X}}_2(k+1|k) &= \mathbf{A}_2 \hat{\mathbf{X}}_2(k|k) \\ \mathbf{P}_2(k+1|k) &= \mathbf{A}_2 \mathbf{P}_2(k|k) \mathbf{A}_2^T + \mathbf{R}_{2W}(k, k) \\ \mathbf{C}_2(k+1) &= \left. \frac{\partial G[k+1, \mathbf{X}_2(k)]}{\partial \mathbf{X}_2(k)} \right|_{\mathbf{X}_2(k)}. \end{aligned}$$

As an example, figure 6 shows the temporal representation

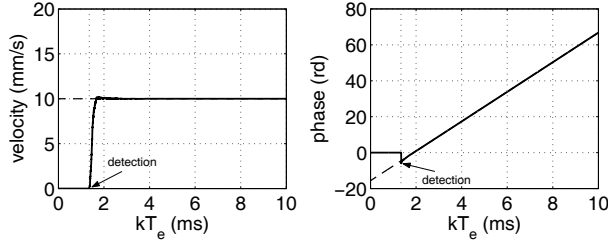


Fig. 6. Estimated velocity (left) and instantaneous phase (right) ($V = 10$ mm/s, SNR = 27 dB).

of the estimated instantaneous phase $\hat{\phi}(k)$ and the estimated particle velocity \hat{V} .

6. RESULTS AND CONCLUSIONS

The detection-estimation scheme, derived in sections 4 and 5, is then compared with the performance of a Phase Derivative Based Estimator (PDBE) and the Cramer-Rao Bound (CRB), described and developed in a previous paper [7]. The PDBE estimator is based on the definition of the instantaneous frequency: $\hat{\phi}(k) = \arctan[y_2(k)/y_1(k)]$. Indeed, particle velocity is given by

$$\hat{V}(k) = \frac{1}{2\pi D} \frac{[\hat{\phi}(k+1) - \hat{\phi}(k-1)]}{2T_e}. \quad (19)$$

The mean of $\hat{V}(k)$, calculated from 1000 samples equally distributed around the time when the amplitude of the signal is maximum, leads to an estimation of the particle velocity \hat{V} . The approximated CRB described in [7]

$$CRB(V) = \frac{1}{2\pi^2} \sqrt{\frac{2}{\pi}} \frac{\beta^3 T_e}{D^2} V_e^3 \frac{1}{SNR} \quad (20)$$

gives the lower bound on the variance of any unbiased estimator [5] of the particle velocity. 700 Monte-Carlo simulations were run on simulated data at various SNR (3 dB, 6 dB, 9 dB, 12 dB, 15 dB, 18 dB, 21 dB, 24 dB, 27 dB, 30 dB,) and for several velocities. Signal parameters were $\beta = 4.6407 \cdot 10^4 \text{ m}^{-1}$, $D = 1.3126 \cdot 10^5 \text{ m}^{-1}$, $K = 1$, $\phi_0 = \pi/7$ and $T_e = 10^{-6} \text{ s}$. The results, shown on figure 7, indicate that EKF results for velocity estimation are very close to CRB, especially when the SNR is high. As can be seen, the EKF turns to be an effective estimator for LDV measurements.

This research work proves that a joint detection-estimation scheme using Kalman filters is a viable solution for particle velocity measurement with a good accuracy. The EKF, although biased, works well in a large range of situations and shows better performance than the PDBE. Moreover, the detection technique, based on a random walk model of

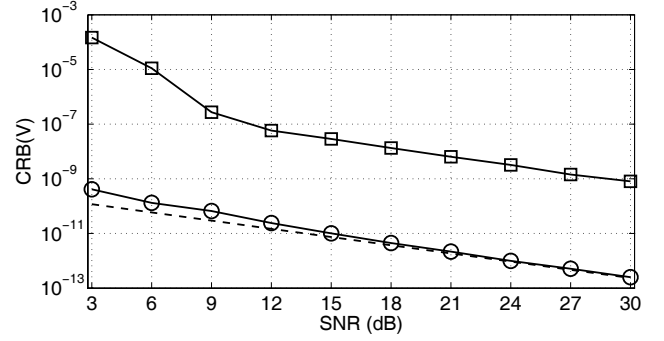


Fig. 7. CRB(V) (---) and variance of EKF (—○—) and PDBE (—□—) estimators versus SNR ($V = 10$ mm/s).

the amplitude of the Doppler signal, does not need an accurate knowledge of the real magnitude and, consequently, is very robust. Especially, this method turns out to be suitable for real-time measurements and may be used in order to design a low-cost integrated laser Doppler sensor.

7. REFERENCES

- [1] O. Besson and F. Galtier, "Estimating Particles Velocity from Laser Measurements: Maximum Likelihood and Cramér-Rao Bounds", *IEEE Transactions on Signal Processing*, 44(12):3056-3068 december 1996.
- [2] F. Durst, A. Melling and J.H. Whitelaw, "*Principles and practice of laser-Doppler anemometry*", Academic Press, 1976,
- [3] S. Haykin, "*Adaptive Filter Theory*", Prentice-Hall, 1991
- [4] R.E. Kalman, "A New Approach to Linear Filtering and Prediction Problems", *Transaction of the ASME - Journal of Basic Engineering*, Vol. 82, march, 1960
- [5] S.M. Kay, "*Fundamentals of statistical signal processing - Estimation theory*", Prentice-Hall, 1993.
- [6] S.M. Kay, "*Fundamentals of statistical signal processing - Detection theory*", Prentice-Hall, 1998.
- [7] A. Le Duff, "*Acoustic Velocity Measurement in the Air by Means of Laser Velocimetry: Cramer-Rao Bounds and Maximum Likelihood Estimation*", in *Proc. IEEE International Conference on Acoustics Speech and Signal Processing, ICASSP'2002*, Orlando, May 2002
- [8] C. Mellet and J.C. Valière, "Maximum likelihood approaches for sound field measurement using LDV", in *Proc. of 10th Int. Symp. on Applications to Laser Techniques to Fluid Mechanics*, Lisbon, July 10-13, 2000.
- [9] J.C. Valière, P. Herzog, V. Valeau and G. Tournois, "Acoustic velocity measurements in the air by means of laser doppler velocimetry : dynamic and frequency range limitations and signal processing improvements", *Journal of Sound and Vibration*, 229(3),607-626, 2000.